

# An Extraction-Free Method for Rapid Detection of CYP2C19 \* 2/3/17 Polymorphisms in One Tube using Melting Curve Analysis

Jianguang Guo<sup>1</sup>, Kangfeng Lin<sup>1</sup>, Weixin You<sup>1</sup>, Qinghan Li<sup>1</sup>, Xiangju Guo<sup>1</sup>, Shuai Wang<sup>1</sup>, Ya Bian<sup>1</sup>, Wenjing Ren<sup>1</sup>, Rui Zhang<sup>2</sup>, Yanping Wang<sup>3</sup>, and Bo-An Li<sup>1</sup>

<sup>1</sup>Xiamen University School of Life Sciences

<sup>2</sup>The First Affiliated Hospital of Xiamen University

<sup>3</sup>Hubei Provincial Hospital of Traditional Chinese Medicine

May 9, 2023

## Abstract

Drug-metabolizing enzymes play an important role in the metabolism of drugs in vivo. Their activity is an important factor affecting the rate of drug metabolism, which directly determines the intensity and persistence of drug action. Patients taking medication can be divided into different metabolic types through detection of CYP2C19 drug-metabolizing enzyme gene polymorphisms, which can then be used for medication guidance for clopidogrel. Here, we describe a detection method based on real-time polymerase chain reaction. This method uses multicolor melting curve analysis to accurately identify different mutation sites and genotypes of CYP2C19 \* 2, CYP2C19 \* 3, and CYP2C19 \* 17. The detection limit of plasmid samples was 1 copies/ $\mu$ l; that of genomic samples was 0.1 ng/ $\mu$ l. The system can detect nine types of CYP2C19 \* 2/3/17 at three sites in one tube, quickly achieving detection within 1 h. Combined with the sample release agent, sample extraction was completed in 5 s, achieving rapid diagnosis without extraction for timely diagnosis and treatment. Furthermore, the system is not limited to blood samples and can also be applied to oropharyngeal and saliva samples, increasing sampling diversity and convenience. When using clinical blood samples (n=93), the detection system we established was able to quickly and accurately identify different genotypes, and the accuracy and effectiveness of the detection were confirmed by Sanger sequencing.

## Introduction

Clopidogrel is an antiplatelet drug widely used in patients with acute coronary syndrome (ACS), including those with non-ST-segment elevation ACS (unstable angina UA or non-Q wave myocardial infarction) and ST-segment elevation myocardial infarction (NSTEMI)(1-3). Specifically, non-ST-segment elevation ACS includes patients with stent implantation after percutaneous coronary intervention, patients with peripheral arterial disease, and patients with recent myocardial infarction or recent ischemic stroke(4-6). Clopidogrel, a prodrug, has no pharmacological activity(7, 8), but active metabolites are mainly produced by the cation of the CYP2C19 enzyme(9-11). The active metabolites produced irreversibly bind to the P2Y12 receptor on the surface of platelets, inhibiting their aggregation and interfering with ADP-mediated platelet activation for an overall antiplatelet effect(12, 13). Genetic variation of the CYP2C19 gene leads to individual differences in CYP2C19 enzyme activity, resulting in four phenotypes: ultrafast metabolizer (UM), fast metabolizer (EM), intermediate metabolizer (IM) and slow metabolizer (PM)(14). CYP2C19 UM patients treated with conventional doses of clopidogrel generate increased levels of active metabolites, with increased platelet inhibition, enhanced antiplatelet function, and increased risk of bleeding(15). Treatment of CYP2C19 PM patients with conventional doses of clopidogrel results in decreased inhibition of platelets, decreased antiplatelet function, and increased risk of thrombosis(16). CYP2C19 \* 2 (rs4244285, c.681G > A) and CYP2C19 \* 3 (rs4986893, c.636G > A) are two major alleles in the Chinese population(17) with frequencies of 23.1% -35% and 2%

-7%, respectively. The CYP2C19 \* 17 (rs12248560, c.-806C > T)-encoded CYP2C19 enzyme displays increased activity, and the frequency of occurrence in the Chinese population is approximately 0.5%-4%(18). In general, methods that detect and distinguish CYP2C19 genotypes should be reliable and rapid, especially when the purpose is for clinical medication guidance, which is related to safety and treatment costs.

Several methods have been developed to detect CYP2C19 gene polymorphisms. However, these methods are almost all performed by highly skilled technicians in well-equipped referral hospitals, and the process is complex and time-consuming. This approach may exclude those who need the medication, which is not helpful for rapid guidance clinically.

Sanger sequencing (referred to as polymerase chain reaction-Sanger sequencing) of PCR-amplified fragments from patient samples is the current 'gold standard' method for detecting CYP2C19 genotypes(19, 20). It facilitates accurate detection of all nucleotide mutations, including new mutations not previously reported. Nonetheless, Sanger sequencing instrumentation is often unaffordable for most local hospitals. In addition, the sequencing process is complex and time-consuming, requiring very careful operation to avoid contamination by PCR amplification. This is also true for other sequencing-based analyses, such as pyrosequencing and next-generation sequencing, as well as analyses based on high-end instruments, such as DNA microchips and mass spectrometry(21). Several simpler and more cost-effective methods have been developed to detect CYP2C19 genotypes(22). Real-time fluorescent quantitative polymerase chain reaction is a good platform for clinical diagnosis because its closed detection format makes it easy to use and fast and reduces the contamination of amplification products(23, 24), and a real-time amplification polymerase chain reaction (PCR) method to detect CYP2C19 genotype polymorphisms has been established(25, 26). However, due to the limited coverage of multiple detection of mutation sites, it is far from practical.

In this study, we developed a detection strategy based on PCR amplification combined with melting curve analysis that uses a combination of adjacent probes and TaqMan probes for amplification. This strategy can detect 9 genotypes of CYP2C19 in a single tube. Here, we describe a new rapid PCR combined with melting curve analysis method for rapid (within 1 h) detection of CYP2C19 \* 2/3/17 sites in one tube. We named this method Rapid PCR Melting Curve Method (RPCR-MC). We systematically evaluated its analytical performance, including mutation detection accuracy, analytical sensitivity, specificity and detection, in clinical samples. We tested the RPCR-MC method by analyzing samples from 93 patients with a high risk of thrombosis after percutaneous coronary intervention(PCI) and compared the results with those of Sanger sequencing.

## Materials and methods

### Construction of plasmid DNA

Gene sequences for CYP2C19\*2, CYP2C19\*3, and CYP2C19\*17 were searched at <https://www.ncbi.nlm.nih.gov/SNP> and downloaded; the 621-bp CYP2C19 \* 2 (rs4244285, c.681G > A) nucleic acid sequence was found, and the mutation site is G - A. Similarly, an 897-bp CYP2C19 \* 3 (rs4986893, c.636G > A) nucleic acid sequence was found, with the mutation site G - A. The 897 -CYP2C19 \* 17 (rs12248560, c.-806C > T) nucleic acid sequence has the mutation site C - T. Additional sequences, CYP2C9 (rs1057910), CYP2C19 \* 4 (rs28399504), CYP2C19 \* 5 (rs56337013), CYP2C19 \* 6 (rs72552267), CYP2C19 \* 7 (rs72558186), and CYP2C19 \* 8 (rs41291556), were designed for specific detection. The designed CYP2C19 \* 2, CYP2C19 \*3, CYP2C19 \*17 wild-type and mutant sequences were synthesized by General Biology; the designed specific sequences were synthesized by Tsingke Biotechnology. The PUC-57 vector with ampicillin resistance was used (see Table S1 for sequence).

Plasmids were diluted in 1X TE (pH 8.0), and the CYP2C19 \* 2 wild-type and CYP2C19 \* 2 mutant plasmids were mixed together with 1:1 to prepare a CYP2C19 \* 2 heterozygous type; the heterozygous plasmids were mixed together with 1:1 to prepare CYP2C19 \* 2/3 heterozygous and CYP2C19 \* 2/17 heterozygous, CYP2C19 \* 3/17 heterozygous and CYP2C19 \* 2/3/17 heterozygous plasmids.

### Clinical samples

A total of 93 blood samples were collected from patients with acute coronary syndrome (ACS/PCI), a high risk of ischemia or a high risk of bleeding at Affiliated Hospital of Xiamen University and store at -20 °C. As controls, oropharyngeal swab samples from 5 healthy individuals and saliva samples of 5 healthy individuals were used.

DNA was extracted from the blood samples, oropharyngeal swab samples and saliva samples using a sample release agent produced by BioDetect (Xiamen) Biotechnology Co., Ltd. For blood, the sample and release agent are used at a ratio of 1:30; for oropharyngeal and saliva, the samples are mixed with the release agent at a ratio of 1:1. The extraction was completed by mixing and shaking for 5 s, and the DNA extracted was used for RPCR-MC, with verification by PCR-Sanger sequencing.

### The RPCR-MC method

Each RPCR-MC analysis reaction mixture contained 1.25  $\mu$ l 5 U/ $\mu$ l D-Taq enzyme, 1  $\mu$ l dNTP Mix (10 mM), 5  $\mu$ l 5XPCR Buffer, 0.3  $\mu$ l 2C19 \* 3-F1 (10  $\mu$ M), 1.2  $\mu$ l 2C19 \* 3-R2 (100  $\mu$ M), 1.2  $\mu$ l 2C19 \* 3-P5 (100  $\mu$ M), 0.25  $\mu$ l 2C19 \* 17-F1 (5  $\mu$ M), 0.1  $\mu$ l 2C19 \* 17-R1 (50  $\mu$ M), 0.1  $\mu$ l 2C19 \* 17-P1 (50  $\mu$ M), 0.1  $\mu$ l 2C19 \* 17-P2 (50  $\mu$ M), 0.3  $\mu$ l 2C19 \* 2-F2 (10  $\mu$ M), 0.12  $\mu$ l 2C19 \* 2-R1 (100  $\mu$ M), 0.12  $\mu$ l 2C19 \* 2-P1 (100  $\mu$ M), 0.12  $\mu$ l 2C19 \* 2-P2 (100  $\mu$ M) mixture, 9.84  $\mu$ l deionized water and 4  $\mu$ l DNA template. 2C19 \* 3 was designed as a TaqMan probe, whereas 2C19 \* 2 and 2C19 \* 17 were designed as adjacent probes. The PCR and melting curve analysis were performed using a SLAN-96S (Shanghai Hongshi) PCR instrument. The PCR involved denaturation at 95°C for 30 s, 45 cycles of 95°C for 2 s and 60°C for 5 s, followed by 72°C for 1 min, 90°C for 1 min, 37°C for 1 min, melting curve analysis was from 45°C to 80°C for 0.06 °C/s.

### Polymerase chain reaction-Sanger sequencing

Each 25- $\mu$ l PCR mixture was prepared as follows: 0.5  $\mu$ l 5 U/ $\mu$ l D-Taq enzyme, 1  $\mu$ l dNTP Mix (10 mM), 5  $\mu$ l 5XPCR Buffer, 1  $\mu$ l 2C19 \* 2-F2 (10  $\mu$ M), 1  $\mu$ l 2C19 \* 2-R1 (10  $\mu$ M), 1  $\mu$ l 2C19 \* 3-F1 (10  $\mu$ M), 1  $\mu$ l 2C19 \* 3-R2 (10  $\mu$ M), 1  $\mu$ l 2C19 \* 17-F1 (10  $\mu$ M), 1  $\mu$ l 2C19 \* 17-R1 (10  $\mu$ M), mixture, 10.5  $\mu$ l deionized water and 2  $\mu$ l DNA template. Conventional PCR was carried out using the SLAN-96S instrument (Shanghai Hongshi) with denaturation at 95°C for 30 s, 45 cycles of 95°C for 2 s and 60°C for 5 s, followed by 72°C for 10 min.

In short, 2  $\mu$ l DNA template was added to a D-Taq enzyme containing 0.5  $\mu$ l 5 U/ $\mu$ l, 1  $\mu$ l dNTP Mix (10 mM), 5  $\mu$ l 5XPCR Buffer, 1  $\mu$ l 2C19 \* 2-F2 (10  $\mu$ M), 1  $\mu$ l 2C19 \* 2-R1 (10  $\mu$ M), 1  $\mu$ l 2C19 \* 3-F1 (10  $\mu$ M), 1  $\mu$ l 2C19 \* 3-R2 (10  $\mu$ M), 1  $\mu$ l 2C19 \* 17-F1 (10  $\mu$ M), 1  $\mu$ l 2C19 \* 17-R1 (10  $\mu$ M) and 10.5  $\mu$ l in deionized water. The amplification conditions were as follows: denaturation at 95°C for 30 s, 45 cycles of 95°C for 2 s 60°C for 5 s, followed by 72°C for 10 min. The amplified products were sent for bidirectional Sanger sequencing.

## Results

### Detection principle flow chart

Through continuous attempts, we finally established a method for rapid detection of 9 genotypes of 3 polymorphic loci in one tube without extraction, which we named RPCR-MC. As shown in Figure 1, the first step is to add the sample to be extracted to the extraction-free reagent at a ratio of 1:30 and simple shock mixing. The whole sample extraction process is simple and fast, requiring only 5 s to complete. Next, the amplification reaction solution is prepared, and the extracted samples are added to the reaction solution for detection. We used asymmetric amplification to amplify the initial template. The ratio of upstream and downstream primers was 1:4. The excess downstream primers will bind with the probe in the melting stage. The designed probe involves two adjacent probes. The 3' end of the first CYP2C19 \* 2 probe is modified with the FAM fluorescent group, the 5' end of the second probe of the adjacent interval 1 base is modified with the BHQ1 quenching group, and the 3' end is modified with phosphate group P to block the extension. Similarly, the fluorophore of the first probe of CYP2C19 \* 17 is ROX, and the quenching group of the second probe is BHQ2. During the study, it was found that the presence of multiple adjacent probes in one tube leads to mutual interference between the primers and probes. However, the method of adjacent probe detection can finally accommodate two polymorphic sites in one tube. Therefore, we combined the Taqman

probe with the adjacent probe. CYP2C19 \* 3 is designed as a TaqMan probe: the 5' end is modified by the HEX fluorophore, and the 3' end carries the BHQ1 quenching group. In the melting heating stage, which is conducted originally under low temperature conditions because the two adjacent probes are close to each other, the fluorescent group and the quenching group interact with each other and do not emit fluorescence. With the gradual increase in temperature, the adjacent probes gradually become separated such that the fluorescent group and the quenching group are separated. For adjacent probes, during the dissolution phase, as the temperature increases, the adjacent fluorophore and quencher separate, thereby releasing fluorescence; For Taqman probes, during the dissolution phase, as the temperature increases, the ability of the probe and template to combine decreases, and gradually falls off the template, that is, from the state of stretching and straightening gradually to the curled state, and the fluorescence intensity changes. As the binding force of the probe and the template chain is reduced with the increase in temperature, a melting peak occurs. Similarly, due to the difference of a base between the homozygous wild-type and mutant samples, the  $T_m$  value is different in the melting stage, and the final test results show different  $T_m$  values.

### Establishment of the detection system

We used the wild-type CYP2C19 \* 2/3/17 plasmid and mutant CYP2C19 \* 2/3/17 plasmid as real samples to simulate wild-type and mutant CYP2C19 \* 2/3/17 genomic sequences, respectively. A primer probe sequence for CYP2C19 \* 2/3/17 type was designed, as shown in Table S2; CYP2C19 \* 3 was designed in the form of a Taqman probe, and CYP2C19 \* 2 and CYP2C19 \* 17 were designed in the form of two adjacent probes. PCR amplification was performed by asymmetric amplification of the upstream and downstream primers. Finally, the optimal detection reaction system was determined, and the detection time was within 1 h. The established reaction system accurately identified and distinguished different sites and genotypes: CYP2C19 \* 2 wild-type and mutant (Figure 2A), CYP2C19 \* 3 wild-type and mutant (Figure 2C), CYP2C19 \* 17 wild-type and mutant (Figure 2E), CYP2C19 \* 2/3 heterozygous (Figure 2B), CYP2C19 \* 2/17 heterozygous (Figure 2D), CYP2C19 \* 3/17 heterozygous (Figure 2F) and CYP2C19 \* 2/3/17 heterozygous (Figure 2G). Based on the experimental results, the system can accurately distinguish different sites and genotypes. Then, we designed sequencing primers, as shown in Table S2, and polymorphic sites were amplified by PCR and sent for Sanger sequencing. The sequencing results are shown in Figure 3: wild-type, mutant and heterozygous CYP2C19 \* 2, respectively, in Figure 3A-C; wild-type, mutant and heterozygous CYP2C19 \* 3, respectively, in Figure 3D-F; and wild-type, mutant and heterozygous CYP2C19 \* 17, respectively, in Figure 3G-I. The sequencing results for the different genotypes of CYP2C19 \* 2/3/17 were consistent with those of RPCR-MC.

### Detection of plasmid sensitivity

After distinguishing multiple sites of CYP2C19 \* 2/3/17 in one tube, we detected the sensitivity of heterozygous samples. First, we prepared CYP2C19 \* 2, CYP2C19 \* 3, CYP2C19 \* 17, and CYP2C19 \* 2/3/17 heterozygous samples and diluted them from  $10^6$  copies/ $\mu$ l to  $10^0$  copies/ $\mu$ l in a 10-fold dilution of 1X TE solution. As depicted in Figure 4A, the detection limit of the CYP2C19 \* 2/3 heterozygous sample was a single copy. Similarly, a single copy was detected for CYP2C19 \* 3 heterozygous samples, CYP2C19 \* 17 heterozygous samples, and CYP2C19 \* 2/3/17 heterozygous samples (Figure 4B-D). Furthermore, we tested the CYP2C19 \* 2/3/17 heterozygous plasmids at 10 copies/ $\mu$ l and 1 copy/ $\mu$ l in a tube to determine the minimum detection limit, as shown in Figure 4E and F. The unique melting temperature  $T_m$  value was obtained as shown in Figure 5. The CYP2C19 \* 2/3/17 hybrid plasmid with 10 copies/ $\mu$ l and 1 copy/ $\mu$ l concentrations was repeatedly detected 9 times, and the average  $T_m$  and standard deviation (SD) of each site were obtained. As indicated in Table S3, the  $T_m$  value of the CYP2C19 \* 2 mutant was 5.6°C higher than that of wild-type, and the  $T_m$  value of the CYP2C19 \* 3 mutant was 4.1°C lower than that of wild-type. The  $T_m$  value of the CYP2C19 \* 17 mutant plasmid was 8.6°C lower than that of wild-type. The results showed that the detection limit of RPCR-MC is 1 copy/ $\mu$ l (or 4 copies per reaction).

### Detection of plasmid specificity

We synthesized mutant plasmids of CYP2C19\*4, CYP2C19\*5, CYP2C19\*6, CYP2C19 \*7, CYP2C19 \*8 and CYP2C9, as shown in Figure 6. The red marker indicates the SNP site of the gene, and the plasmid

was diluted with 1X TE solution to a concentration of  $10^3$  copies/ $\mu$ l. The results were analyzed by the RPCR-MC detection system. Only CYP2C19 \* 2/3/17 heterozygous mutant samples were detected, and each site had a single correct  $T_m$  value; Conversely, the other types of samples were not detected, showing that the detection system we established has good specificity.

### Determination of blood sample sensitivity

We extracted human blood samples 1 and 2 using a commercial blood magnetic bead extraction kit produced by BioDetect (Xiamen) Biotechnology Co., Ltd. and diluted them with a 10-fold gradient of 1X TE to obtain 1 ng/ $\mu$ l and 0.1 ng/ $\mu$ l samples. Each sample was independently tested five times, and the minimum detection limit of the blood sample genome was 0.1 ng/ $\mu$ l, as shown in Figure 7A-F. Among them, CYP2C19 \* 2 in blood 1 sample was homozygous wild-type, CYP2C19 \* 3 was heterozygous, and CYP2C19 \* 17 was homozygous wild-type; in blood 2 sample, CYP2C19 \* 2 was heterozygous, CYP2C19 \* 3 was homozygous, and CYP2C19 \* 17 was homozygous. We also detected 5 oropharyngeal samples and 5 saliva samples. For the oropharyngeal swabs, both sides of the mouth were gently sampled. The swabs with exfoliated oral cells were placed in the sample release agent, and the samples were shaken and mixed. For saliva, a collection tube was used; the sample was mixed with the release agent in equal proportion and shaken evenly for detection. The results for the oropharyngeal samples are shown in Figure S1A. Three cases of CYP2C19 \* 2 heterozygosity, one case of CYP2C19 \* 2 homozygous wild-type, one case of CYP2C19 \* 2 homozygous mutation, five cases of CYP2C19 \* 3 homozygous wild-type and five cases of CYP2C19 \* 17 homozygous wild-type were successfully detected. The results for the saliva samples are shown in Figure S1B. Three cases of CYP2C19 \* 2 heterozygosity, 2 cases of CYP2C19 \* 2 homozygous wild-type, 1 case of CYP2C19 \* 3 heterozygosity, 4 cases of CYP2C19 \* 3 homozygous wild-type and 5 cases of CYP2C19 \* 17 homozygous wild-type were successfully detected. Specific single peaks at each site were accurately observed.

### Detection of clinical samples

A total of 93 blood samples were collected from the First Affiliated Hospital of Xiamen University. All samples were detected by RPCR-MC in an extraction-free manner. The results were consistent with the results of Sanger sequencing, as shown in Table S4. Figure 8 illustrates that CYP2C19 \* 2 heterozygosity and wild-type account for a relatively high proportion of the Chinese population, with homozygous mutation being relatively rare. CYP2C19 \* 3 wild-type accounts for a relatively high proportion of the population tested, heterozygosity was less common, and mutation was the least common. CYP2C19 \* 17 mostly comprised wild-type, with mutant and heterozygosity being almost absent. These results indicate that the polymorphism ratio of each locus in the Chinese population is roughly consistent with previous research results.

### Discussion

We developed a method for rapid identification of CYP2C19 \* 2/3/17 polymorphisms and named it RPCR-MC. With the continuous progress medical science development, many drugs are reported in the world but later removed from research because of adverse reactions(27). In general, drug efficacy and adverse reactions are related to ethnic and individual differences associated with genetic differences between people(28). Single-nucleotide polymorphism involves a difference in one base(29). There are several kinds of genome sequence differences, with SNPs being the most common, which is of great clinical significance. When patients with the same disease take the same drugs, some may have different reactions, and drugs are divided into significantly effective, effective, and ineffective. In clinical treatment, doctors usually cannot determine which drugs are most effective according to the patient's symptoms and must rely on average statistical results of clinical research data and personal experience for decision-making. Moreover, patients with the same symptom or disease may have different treatment outcomes, even with the same drug, and this difference can be predicted by SNP detection. An SNP may alter the amino acid sequence of the expressed protein, which may change the target site of a drug, with decreases in or lack of affinity. Therefore, SNP analysis can help to achieve correct diagnosis and effective treatment. As a detection system for CYP2C19 \* 2/3/17, an important gene for guiding clopidogrel use, RPCR-MC can accurately distinguish different CYP2C19 \* 2, CYP2C19 \* 3

and CYP2C19 \* 17 types. Based on detection of different sample concentrations, the detection limit of the method was determined to be 1 copy/ $\mu$ l, and the detection limit for the blood genome was 0.1 ng/ $\mu$ l, indicating high detection sensitivity.

Some traditional methods for detecting SNPs, such as dideoxy sequencing, pyrosequencing, and whole-genome sequencing, can reveal important features required for SNP typing, such as the type of SNP and its accurate location. However, this method is cumbersome, expensive, and not suitable for general use. In addition, SSCP occurs when single-stranded DNA forms a secondary structure under neutral conditions, and different secondary structures exhibit different mobilities by electrophoresis. The disadvantage of this method is that the mutation type and specific location cannot be determined. Hybridization sequencing-chip sequencing technology is based on imprinting hybridization or nucleic acid in situ hybridization, in which an oligonucleotide probe hybridizes with the target DNA; the fluorescent group carried by the oligonucleotide probe marks the DNA and identifies the specific sequence. Nevertheless, there are some issues with this kind of technology: as it is difficult to identify nonspecific signals through only a single hybridization, it may lead to sequence misreading due to some nonspecific hybridization. In addition, the chip is expensive, as is the equipment required, which is not conducive to universal application. According to the  $T_m$  value analysis system established in this study, which recognizes the target sequence using specific primers and probes for PCR amplification and then analyzes the  $T_m$  value through melting curve analysis, our system has high specificity and can accurately identify a single-base mutation in the target gene in a complex mixture. Furthermore, RPCR-MC is easy to operate, and the sample release agent is used for biological samples without extraction, reducing the cumbersome process of extracting sample nucleic acids. The detection time is also short and completed within 1 h, and it has high-throughput multiple detection capabilities. Indeed, RPCR-MC can detect 9 genotypes of 3 sites in a single tube.

Recent studies have shown that the determination of SNPs between different population groups can effectively identify the target molecules of new drugs. Due to SNP differences between patients, such findings can be used to reduce adverse reactions to known drugs and clinical trial drugs as well as improve their efficacy. In addition, beneficial drugs that have been eliminated due to adverse reactions may be revisited; as long as the associated SNP is found, such effective drugs can be used in clinical practice. Therefore, quickly and accurately identifying a single-base mutation is particularly important. In view of the rapid and convenient, high sensitivity and good specificity of the RPCR-MC detection system, this method will improve detection efficiency by medical staff, reduce workloads, and play an important role in the early recovery of patient health. Regardless of the time cost or test reagent cost, our detection system is the best choice.

In conclusion, we have developed a method for identifying the CYP2C19 \* 2/3/17 locus, which is helpful for guiding the use of clopidogrel.

### **Acknowledgments**

National Key Research and Development Program of China (2020YFA0112300 to B.-A.L.), the National Natural Science Foundation of China (grant number 81972458 to B.-A.L. 82103092 to R.Z.), the Natural Science Foundation of Fujian Province (grant number 2022J05312 to R.Z.) the Health-Education joint research project of Fujian province (grant numbers 2019-WJ-34 to B.-A.L. and Z.-M.Z.), and “Project 111” sponsored by the State Bureau of Foreign Experts and Ministry of Education (grant number B06016).

### **Declaration of Interest Statement**

The authors declare that they have no known competing financial interests or personal relationships that could have appeared to influence the work reported in this paper.

### **REFERENCES**

1. Xiao Z, and Theroux P. Clopidogrel inhibits platelet-leukocyte interactions and thrombin receptor agonist peptide-induced platelet activation in patients with an acute coronary syndrome. 2004;43:1982-8.
2. Wakabayashi S, Kitahara H, Nishi T, Sugimoto K, Nakayama T, Fujimoto Y, et al. Platelet inhibition

- after loading dose of prasugrel in patients with ST-elevation and non-ST-elevation acute coronary syndrome. *Cardiovascular intervention and therapeutics*. 2018;33(3):239-46.
3. Lee S, Vargova K, Hizoh I, Horvath Z, Gulacsi-Bardos P, Sztupinszki Z, et al. High on clopidogrel treatment platelet reactivity is frequent in acute and rare in elective stenting and can be functionally overcome by switch of therapy. 2014;133:257-64.
  4. Pinxterhuis TH, Ploumen EH, Zocca P, Doggen CJM, Schotborgh CE, Anthonio RL, et al. Outcome after percutaneous coronary intervention with contemporary stents in patients with concomitant peripheral arterial disease: A patient-level pooled analysis of four randomized trials. *Atherosclerosis*.2022;355:52-9.
  5. Khalid U, Bandevali S, Jones PG, Virani SS, Hira R, Hamzeh I, et al. Prescription Patterns of Clopidogrel, Prasugrel, and Ticagrelor After Percutaneous Coronary Intervention With Stent Implantation (from the NCDR PINNACLE Registry).*Am J Cardiol*. 2019;124(12):1807-12.
  6. Sasaki M, Mitsutake Y, Ueno T, Fukami A, Sasaki KI, Yokoyama S, et al. Low ankle brachial index predicts poor outcomes including target lesion revascularization during the long-term follow up after drug-eluting stent implantation for coronary artery disease. *J Cardiol*. 2020;75(3):250-4.
  7. Sidhu MS, Lyubarova R, Bangalore S, and Bonaca MP. Challenges of long-term dual antiplatelet therapy use following acute coronary syndromes. *American heart journal*.2022;246:44-64.
  8. Bolognese L, and Angiolillo DJ. Unravelling the benefit against the risk of long-term dual antiplatelet therapy. *Current opinion in cardiology*. 2011;26 Suppl 1:S22-30.
  9. Ryu SH, Park BY, Kim SY, Park SH, Jung HJ, Park M, et al. Regioselective hydroxylation of omeprazole enantiomers by bacterial CYP102A1 mutants. *Drug metabolism and disposition: the biological fate of chemicals*. 2014;42(9):1493-7.
  10. Kang D, Geng T, Lian Y, Li Y, Ding G, Huang W, et al. Direct inhibition of Re Du Ning Injection and its active compounds on human liver cytochrome P450 enzymes by a cocktail method. *Biomed Chromatogr*. 2017;31(7).
  11. Brosen K. Pharmacogenetics of drug oxidation via cytochrome P450 (CYP) in the populations of Denmark, Faroe Islands and Greenland. *Drug metabolism and personalized therapy*. 2015;30(3):147-63.
  12. Garcia C, Maurel-Ribes A, Nauze M, N'Guyen D, Martinez LO, Payrastra B, et al. Deciphering biased inverse agonism of cangrelor and ticagrelor at P2Y12 receptor. *Cell Mol Life Sci*. 2019;76(3):561-76.
  13. Wu CC, Tsai FM, Chen ML, Wu S, Lee MC, Tsai TC, et al. Antipsychotic Drugs Inhibit Platelet Aggregation via P2Y 1 and P2Y 12 Receptors. *Biomed Res Int*.2016;2016:2532371.
  14. Mwinyi J, Vokinger K, Jetter A, Breitenstein U, Hiller C, Kullak-Ublick GA, et al. Impact of variable CYP genotypes on breast cancer relapse in patients undergoing adjuvant tamoxifen therapy. *Cancer chemotherapy and pharmacology*.2014;73(6):1181-8.
  15. Braun OO, Angiolillo DJ, Ferreiro JL, Jakubowski JA, Winters KJ, Effron MB, et al. Enhanced active metabolite generation and platelet inhibition with prasugrel compared to clopidogrel regardless of genotype in thienopyridine metabolic pathways. *Thrombosis and haemostasis*. 2013;110(6):1223-31.
  16. Xie X, Ma YT, Yang YN, Li XM, Ma X, Fu ZY, et al. CYP2C19 phenotype, stent thrombosis, myocardial infarction, and mortality in patients with coronary stent placement in a Chinese population. *PloS one*. 2013;8(3):e59344.
  17. Goh LL, Lim CW, Sim WC, Toh LX, and Leong KP. Analysis of Genetic Variation in CYP450 Genes for Clinical Implementation. *PloS one*. 2017;12(1):e0169233.
  18. Barter ZE, Tucker GT, and Rowland-Yeo K. Differences in cytochrome p450-mediated pharmacokinetics between chinese and caucasian populations predicted by mechanistic physiologically based pharmacokinetic

modelling. *Clinical pharmacokinetics*. 2013;52(12):1085-100.

19. Huang X, Zhou Y, Zhang J, Xiang H, Mei H, Liu L, et al. The importance of CYP2C19 genotype in tacrolimus dose optimization when concomitant with voriconazole in heart transplant recipients. *British journal of clinical pharmacology*. 2022.

20. Chambliss AB, Resnick M, Petrides AK, Clarke WA, and Marzinke MA. Rapid screening for targeted genetic variants via high-resolution melting curve analysis. *Clin Chem Lab Med*. 2017;55(4):507-16.

21. Yang L, George J, and Wang J. Deep Profiling of Cellular Heterogeneity by Emerging Single-Cell Proteomic Technologies. *Proteomics*. 2020;20(13):e1900226.

22. Jabir FA, and Hoidy WH. Pharmacogenetics as Personalized Medicine: Association Investigation of SOD2 rs4880, CYP2C19 rs4244285, and FCGR2A rs1801274 Polymorphisms in a Breast Cancer Population in Iraqi Women. *Clin Breast Cancer*.2018;18(5):e863-e8.

23. Mortarino M, Franceschi A, Mancianti F, Bazzocchi C, Genchi C, and Bandi C. [Quantitative PCR in the diagnosis of Leishmania]. *Parassitologia*.2004;46(1-2):163-7.

24. Bretagne S. Primary diagnostic approaches of invasive aspergillosis—molecular testing. *Med Mycol*. 2011;49 Suppl 1:S48-53.

25. Kwong KM, Tam CC, Chan R, Lee SWL, Ip P, and Kwok J. Comparison of Single Nucleotide Polymorphism genotyping of CYP2C19 by Loop-mediated isothermal amplification and real-time PCR melting curve analysis. *Clin Chim Acta*.2018;478:45-50.

26. Krajciova L, Petrovic R, Deziova L, Chandoga J, and Turcani P. Frequency of selected single nucleotide polymorphisms influencing the warfarin pharmacogenetics in Slovak population. *Eur J Haematol*. 2014;93(4):320-8.

27. Cooper JW. Adverse drug reaction-related hospitalizations of nursing facility patients: a 4-year study. *South Med J*. 1999;92(5):485-90.

28. Freitas AR, Tedim AP, Novais C, Lanza VF, and Peixe L. Comparative genomics of global *optrA*-carrying *Enterococcus faecalis* uncovers a common chromosomal hotspot for *optrA* acquisition within a diversity of core and accessory genomes. *Microb Genom*. 2020;6(6).

29. Zhang Y, Xu L, Qiu J, Li Z, Li L, Ren G, et al. Association between SNP rs10569304 on the second expressed region of hole gene and the congenital heart disease. *J Huazhong Univ Sci Technolog Med Sci*. 2010;30(4):430-6.

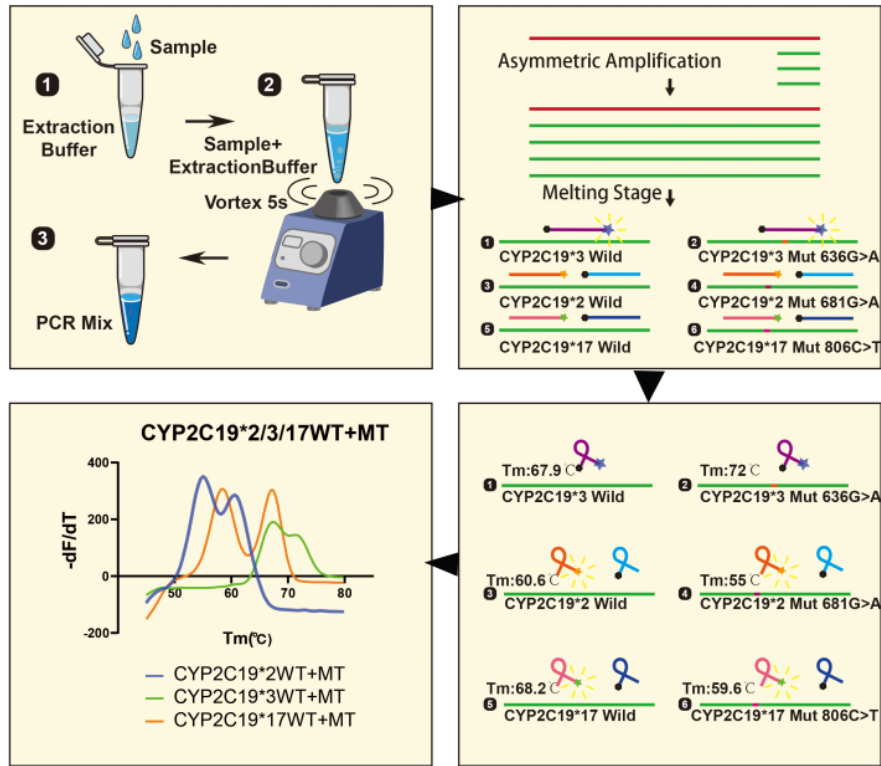


**FIG 1 RPCR-MC detection principle flow chart.** From left to right, the sample was first extracted, and the sample and release agent were combined and mixed well. In the amplification stage, the initial sample is amplified by asymmetric amplification using upstream and downstream primers. Then, with the increase in temperature in the melting stage, the fluorescent groups and quenching groups of the probe become separated, and the binding ability of the probe to the template is reduced, resulting in a specific  $T_m$  value and forming a melting peak diagram. WT, wild-type; MT, mutant; W+M, heterozygosity.

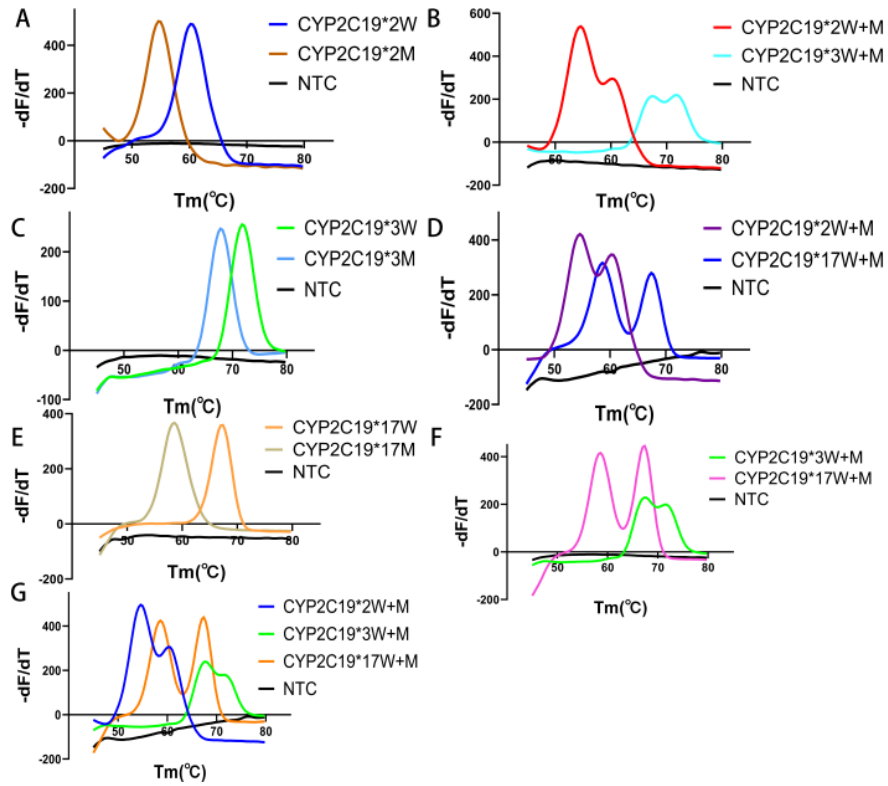


**FIG 2 Identification of CYP2C19 \* 2/3/17 polymorphism loci.** A. CYP2C19 \* 2 wild-type and mutant. B. CYP2C19 \* 2/3 heterozygosity. C. CYP2C19 \* 3 wild-type and mutant. D. CYP2C19 \* 2/17 heterozygosity. E. CYP2C19 \* 17 wild-type and mutant. F. CYP2C19 \* 3/17 heterozygosity. G. CYP2C19 \* 2/3/17 heterozygosity. W, wild-type; M, mutant; -dF/dt, negative derivative of fluorescence over temperature; NTC, negative control.

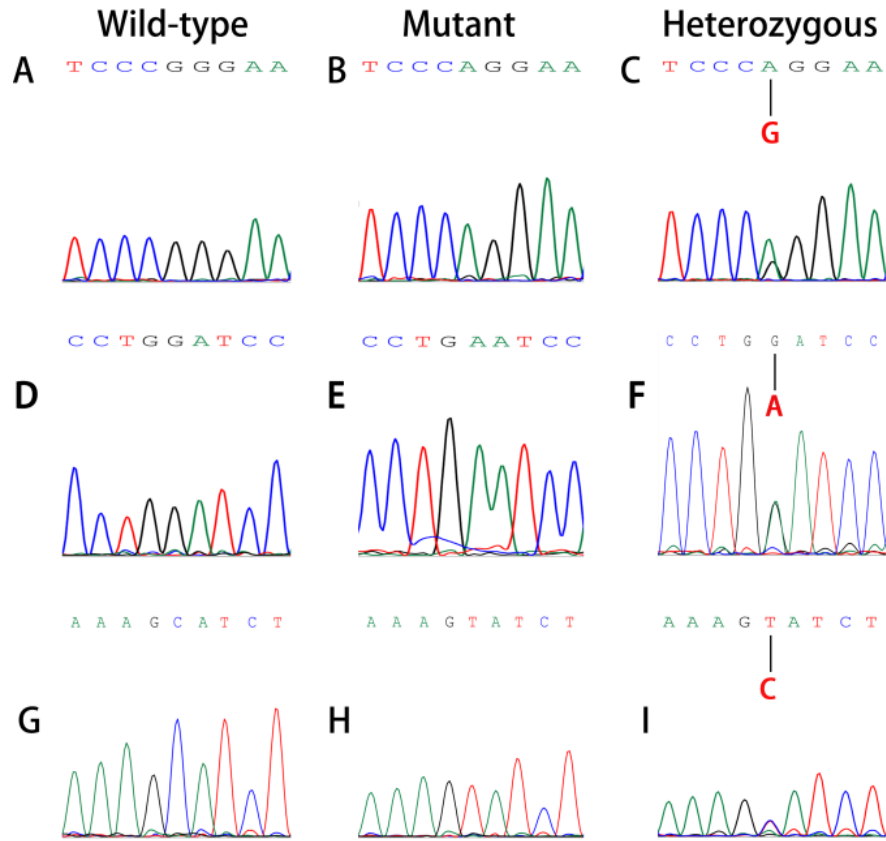


**FIG 3 Sanger sequencing results for CYP2C19 \* 2/3/17 polymorphism.** A-C. CYP2C19 \* 2 wild-type, mutant and heterozygosity. D-F. CYP2C19 \* 3 wild-type, mutant and heterozygosity. G-I. CYP2C19 \* 17 wild-type, mutant and heterozygosity.

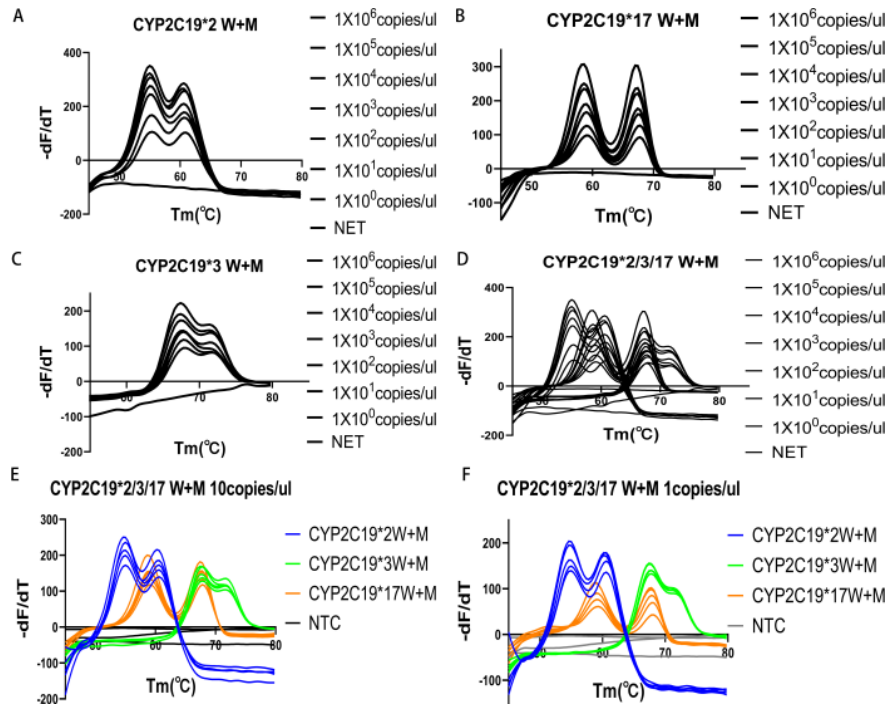


**FIG 4 Plasmid detection limits for CYP2C19 \* 2/3/17 polymorphisms.** A. The detection limit of CYP2C19 \* 2 heterozygosity is 1 copy/ $\mu$ l. B. The detection limit of CYP2C19 \* 17 heterozygosity is 1 copy/ $\mu$ l. C. The detection limit of CYP2C19 \* 3 heterozygosity is 1 copy/ $\mu$ l. D. The detection limit of CYP2C19 \* 2/3/17 heterozygosity is 1 copies/ $\mu$ l. E. CYP2C19 \* 2/3/17 heterozygous plasmid 10 copies/ $\mu$ l independent repeat 5 groups (n = 5). F. CYP2C19 \* 2/3/17 heterozygous plasmid 1 copies/ $\mu$ l independently repeated 5 groups (n = 5). W, wild-type; M, mutant; W+M, heterozygosity. -dF/dT, negative derivative of fluorescence over temperature; NTC, negative control.

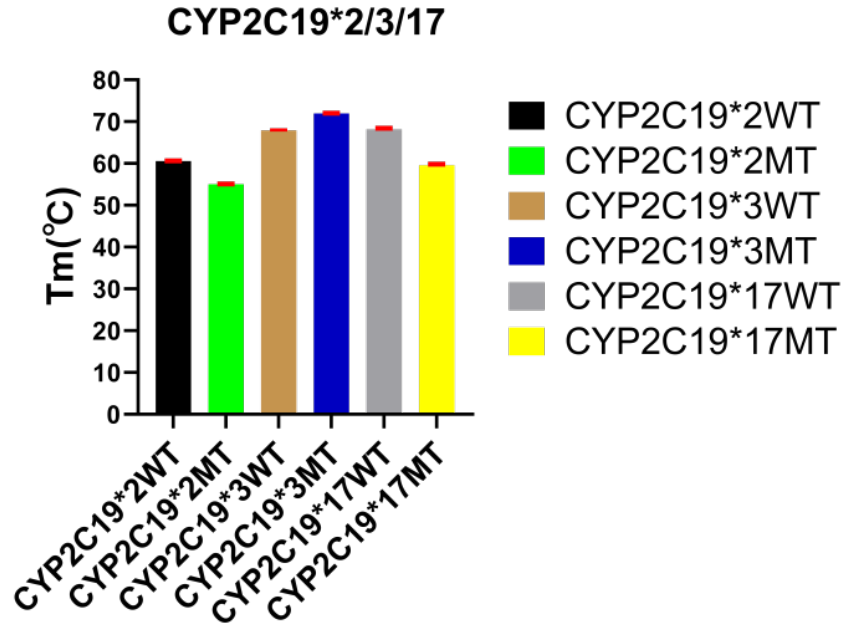


**FIG 5 Tm values for CYP2C19 \* 2/3/17 polymorphisms.** CYP2C19 \* 2, CYP2C19 \* 3, CYP2C19 \* 17 wild-type and mutant all had unique Tm values in 9 independent repeated tests of 10 copies/ $\mu$ l and 1 copies/ $\mu$ l plasmid samples, n=9, P<0.0001. WT, wild-type; MT, mutant.

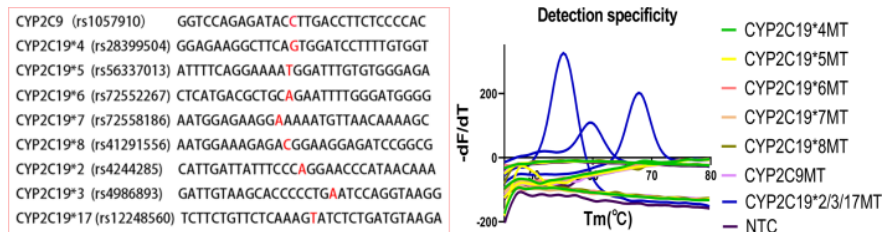


**FIG 6 Specificity of the RPCR-MC system.** CYP2C19 \* 4-8, CYP2C9-related specific sequences synthesized are on the left, red-labeled bases represent the mutation site of the sequence, the right side is the melting curve analysis results, MT, mutant. NTC, negative control.

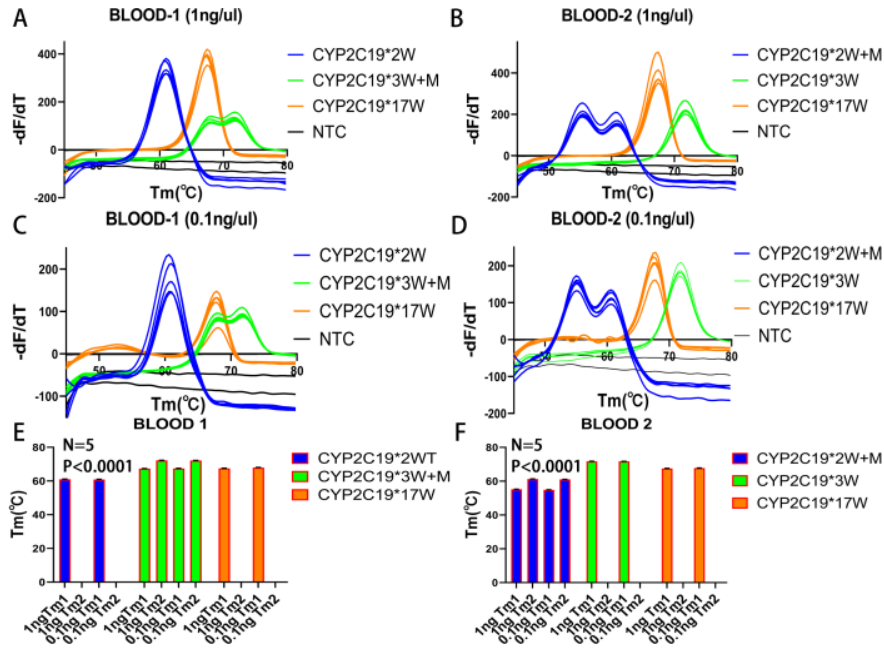


**FIG 7 Detection limit for blood genomic samples.** A, B are 1 ng/ul blood 1 and blood 2 samples, respectively, tested 5 times independently (n = 5). C, D. 0.1 ng/ul of blood 1 and blood 2 samples, respectively, independently repeated 5 times (n = 5). E, F. Repeated test difference analysis of Tm values for blood 1 and blood 2 samples, respectively. WT, wild-type; MT, mutant. NTC, negative control.

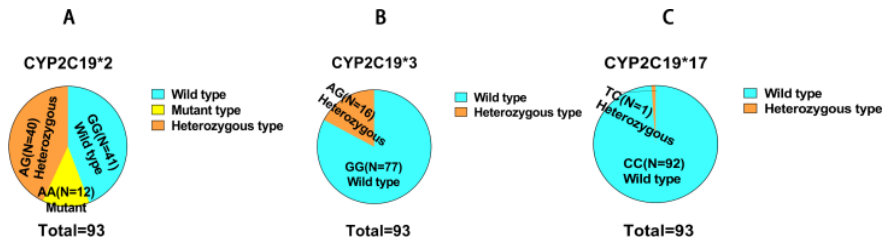


**FIG 8 Detection of clinical samples with the RPCR-MC system.** A. CYP2C19 \* 2 detection, 41 wild-type samples, 12 mutant samples, and 40 heterozygous samples. B. CYP2C19 \* 3 detection, 77 wild-type samples, 0 mutant samples, 16 heterozygous samples. C. CYP2C19 \* 17 detection, 92 wild-type samples, 0 mutant samples, and 1 heterozygous sample. (total number, 93).

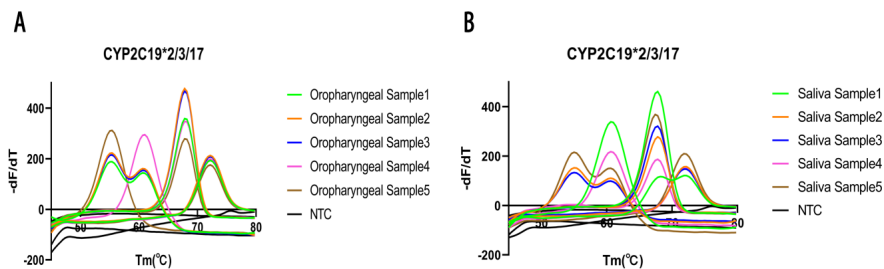


**Figure S1. Oropharyngeal and saliva samples were detected by the RPCR-MC system.** A. Oropharyngeal swab samples were prepared by the extraction-free method, and 5 oropharyngeal swab samples

were randomly detected to detect the CYP2C19 \* 2/3/17 sites. B. Saliva samples were prepared by the extraction-free method, and 5 saliva samples were randomly processed to detect CYP2C19 \* 2/3/17 sites. -dF/dt, negative derivative of fluorescence over temperature.

Table S1. The Sequences of CYP2C19\*2/3/17 ,CYP2C9 and CYP2C19\*4-8 Used in Different Experiments

Gene name
CYP2C19*2(rs4244285,c.681G>A) WT CYP2C19*2(rs4244285,c.681G>A) MT CYP2C19*3(rs4986893,c.636G>A)WT CYP2C19*3(rs4986893,c.636G>A) MT

WT, wild type.

MT, mutant type.

Red markers indicate mutation sites.

Table S2. The Sequences of Primers and Probes Used in Different Methods

SNPs	Methods
rs4244285 rs4986893 rs12248560	Adjacent probe Forward primer Reverse primer Probe1 Probe2 Sequencing Forward prim

FAM, 6-carboxyfluorescein; HEX, hexachloro-6-carboxyfluorescein; ROX,6-Carboxy-X-rhodamine

Table S3. Tm for each plasmid and [?]<sub>c</sub>Tm between wild-type plasmid and mutant plasmid

SNPs	Mutation site	Tm±2SDs (°C)	Tm±2SDs (°C)	[?] <sub>c</sub> Tm <sub>c</sub>
		WT(n =9) MT(n =9)	WT(n =9) MT(n =9)	
rs4244285 rs4986893 rs12248560	G>A A T	60.6±0.16 67.9±0.24 68.2±0.5	55.0±0.2 72.0±0.12 59.6±0.48	5.6±0.1

WT, wild type.

MT, mutant type.

[?]<sub>c</sub>Tm<sub>c</sub> Tm for wild type - Tm for mutant type.

Table S4. Mutations detected by RPCR-MC and PCR Sanger sequencing in 93 clinical samples from population in China

SNPs	Mutation site	Detected by:	Detected by:
		RPCR-MC Sequencing WT MT HT WT MT HT	RPCR-MC Sequencing WT MT HT WT MT HT
rs4244285 rs4986893 rs12248560	G>A G>A C>T	41 12 40 77 0 16 92 0 1	41 12 40 77 0 16 92 0 1

WT, wild type.

MT, mutant type.

HT, heterozygous type.